Mineralogical Magazine, June 2010, Vol. 74(3), pp. 567–575

The crystal structure of zigrasite, $MgZr(PO_4)_2(H_2O)_4$, a heteropolyhedral framework structure

F. C. HAWTHORNE[1,]* AND W. B. SIMMONS[2]

[1] Department of Geological Sciences, University of Manitoba, Winnipeg, Manitoba R3T 2N2, Canada
[2] Department of Earth and Environmental Sciences, University of New Orleans, New Orleans, Louisiana 70148, USA

[*Received 28 April 2010; Accepted 1 July 2010*]

ABSTRACT

The crystal structure of zigrasite, ideally $MgZr(PO_4)_2(H_2O)_4$, *a* 5.3049(2), *b* 9.3372(4), *c* 9.6282(5) Å, α 97.348(1)º, β 91.534(1)º, γ 90.512(4)º, *V* 472.79(5) Å^3, Z = 2, triclinic, *P*1, $D_{calc.}$ 2.66 g.cm^{-3}, from the giant 1972 pocket at Newry, Oxford County, Maine, USA, has been solved and refined to R_1 3.75% on the basis of 2623 unique reflections ($F_o > 4\sigma F$). There are two *P* sites, each of which is solely occupied by P with <P−O> distances of 1.532 and 1.533 Å, respectively. There are two *Mg* sites, both of which are occupied by Mg and are octahedrally coordinated two O anions and four (H_2O) groups with <Mg−O> distances of 2.064 and 2.075 Å, respectively. There is one *Zr* site, occupied by Zr and octahedrally coordinated by six O anions with a <Zr−O> distance of 2.065 Å. The (ZrO_6) octahedron shares corners with six (PO_4) tetrahedra, forming a $[Zr(PO4)_2]$ sheet parallel to (001). These sheets are stacked in the *c* direction and linked by $(MgO_2(H_2O)_4)$ octahedra that share O atoms with the (PO_4) groups. The structure is formally a heteropolyhedral framework structure, but the linkage is weaker in the *c* direction, accounting for the marked (001) cleavage.

KEYWORDS: zigrasite, phosphate, crystal structure, Newry pegmatite, Maine, malhmoodite

Introduction

ZIGRASITE, $MgZr(PO_4)_2(H_2O)_4$, was described as a new mineral from the giant 1972 gem tourmaline-bearing pocket at the Dunton Quarry, Newry, Oxford County, Maine, USA, by Hawthorne *et al.* (2009). It occurs as complex aggregates of three distinct phases, zigrasite and two unnamed phases: the Ca analogue of zigrasite, $CaZr(PO_4)_2(H_2O)_4$, and $Zr(PO_3OH)_2(H_2O)_4$. Zigrasite is associated with tourmaline, microcline, quartz, albite, beryl, amblygonite-montebrasite, childrenite-eosphorite and apatite, and crystallized as one of the last minerals during pocket formation.

Experimental details

The single crystal of zigrasite used in this work, a pale tan fragment with dimensions 25 mm × 60 μm × 100 μm, was removed from a polished thin section. Electron microprobe analysis subsequent to collection of the X-ray intensity data showed it to be uniform and close to end-member composition. The crystal used for structure determination was analysed, using a Cameca SX-100 electron-microprobe, by Hawthorne *et al.* (2009). Determination of the crystal structure (see below) shows that zigrasite contains four (H_2O) groups per formula unit, and the empirical formula for zigrasite was calculated on the basis of 12 anions including 4 (H_2O) groups per formula unit: $(Mg_{0.97}Fe^{2+}_{0.01}Zn_{0.01})_{\Sigma=0.99}(Zr_{0.99}Hf_{0.01})_{\Sigma=1.00}P_{2.00}O_8(H_2O)_4$, ideally $MgZr(PO_4)_2(H_2O)_4$.

---

* E-mail: frank_hawthorne@umanitoba.ca
DOI: 10.1180/minmag.2010.074.3.567

Data collection and crystal-structure refinement

The single crystal of zigrasite was mounted on a Bruker AXS SMART APEX diffractometer equipped with a CCD detector and using Mo-$K\alpha$ radiation. The intensities of 5497 reflections were collected to 60º2θ using 30 s per 0.2º frame, and an empirical absorption correction (*SADABS*, Sheldrick, 1998) was applied. The refined unit-cell parameters for the triclinic cell (Table 1) were obtained from 6768 reflections with $I > 10\sigma$. The crystal structure of zigrasite was solved by direct methods with the Bruker *SHELXTL* Version 5.1 system of programs (Sheldrick, 1997) and refined in space group $P\bar{1}$ to $R_1 = 3.65\%$ and a GooF of 1.018. Refinement of the structure was based on 2623 intensities of unique observed reflections ($F_o > 4\sigma F$). Scattering curves for neutral atoms were taken from the *International Tables for X-ray Crystallography* (1992). *R* indices are given in Table 1, and are expressed as percentages. Details of the data collection and structure refinement are given in Table 1, final atom parameters are given in Table 2, selected interatomic distances and angles in Table 3, and bond-valence values in Table 4. A list of observed and calculated structure factors has been deposited with the Principal Editor of *Mineralogical Magazine* and is available from www.minersoc.org/pages/e_journals/dep_mat.html.

Description of the structure

Atom coordination

There are two *P* sites, each of which is solely occupied by P and tetrahedrally coordinated by four O anions with <P–O> distances of 1.532 and 1.533 Å, respectively, close to the grand <P–O> distance in minerals of 1.537 Å given by Huminicki and Hawthorne (2002). There are two *Mg* sites, both of which are occupied solely by Mg and are octahedrally coordinated by two O anions and four (H_2O) groups with <Mg–O> distances of 2.064 and 2.075 Å, respectively. There is one *Zr* site, solely occupied by Zr and octahedrally coordinated by six O anions with a <Zr–O> distance of 2.065 Å.

There are 12 anion sites in the structure of zigrasite (Table 2), labelled O(1) to O(12). The incident bond-valence sums from the P, Mg and Zr cations in the structure to these anions fall into two groups: O(1) to O(8) lie between 1.64 and 2.00 v.u. (valence units) and O(9) to O(12) lie between 0.30 and 0.42 v.u. (Table 4). Accordingly, O(1)–O(8) are assigned as O anions and O(9)–O(12) are assigned as (H_2O) groups. In accord with this assignment, eight H atoms were located at the final stages of structure refinement and their parameters were refined with the soft constraint that the O(donor)–H distance be close to 0.98 Å. The stereochemistry of the resulting hydrogen-bond arrangement is given in Table 3.

Structure topology

The Zr octahedron shares corners with six (PO_4) tetrahedra to form a pinwheel cluster (Moore 1973) that we may express in its most general form as $[^{[6]}M(^{[4]}TO_4)_6]$. In zigrasite, this cluster forms a fragment of a $[Zr(PO_4)_2]$ sheet (Fig. 1)

TABLE 1. Miscellaneous information for zigrasite.

a (Å)	5.3049(2)	Crystal size (μm)	2560 × 100
b	9.3372(4)	Radiation/monochromator	Mo-$K\alpha$ / graphite
C	9.6282(4)	No. of reflections	14396
α (º)	97.348(1)	No. in Ewald sphere	5497
β	91.534(1)	No. unique reflections	2766
γ	90.512(1)	No. $F_o > 5\sigma(F)$	2623
V (Å^3)	472.79(5)	R_{merge} %	1.6
Space group	$P\bar{1}$	R_1 %	3.75
Z	2	wR_2 %	8.72
D_{calc} (g/cm^3)	2.66		
Cell content	2 $[Zr(PO_4)_2Mg(H_2O)_4]$		
$R_1 = \Sigma(F_o - F_c) / \Sigma F_o$			
$wR_2 = [\Sigma wF_o - F_c)^2 / \Sigma w\ F_o^2\ ]^{½}$, $w = 1$			

TABLE 2. Atom positions and displacement paramters (Å^2) for zigrasite.

	x	y	z	U_{eq}	U_{11}	U_{22}	U_{33}	U_{23}	U_{13}	U_{12}
Zr	0.25362(4)	0.74773(3)	0.49040(2)	0.00794(9)	0.00537(13)	0.00899(13)	0.00943(13)	0.00079(8)	−0.00038(8)	−0.00084(8)
P(1)	0.26500(14)	0.45008(8)	0.68108(8)	0.0129(2)	0.0104(3)	0.0144(3)	0.0137(3)	0.0016(3)	−0.0005(3)	−0.0010(3)
P(2)	0.23232(14)	0.06111(8)	0.32252(8)	0.0123(2)	0.0102(3)	0.0132(3)	0.0133(3)	0.0014(3)	−0.0003(2)	−0.0013(3)
Mg(1)	0	0	0	0.0185(3)	0.0126(7)	0.0290(8)	0.0139(7)	0.0030(6)	−0.0010(5)	−0.0030(6)
Mg(2)	½	½	0	0.0199(3)	0.0179(7)	0.0242(8)	0.0168(7)	0.0004(6)	−0.0017(6)	−0.0002(6)
O(1)	0.3139(5)	0.5903(3)	0.6181(3)	0.0234(5)	0.0225(12)	0.0209(11)	0.0280(12)	0.0073(9)	0.0006(9)	−0.0004(9)
O(2)	0.2402(4)	0.4846(3)	0.8389(2)	0.0197(5)	0.0173(11)	0.0272(12)	0.0140(10)	0.0010(8)	−0.0005(8)	0.0020(9)
O(3)	0.4845(4)	0.3458(3)	0.6475(2)	0.0195(5)	0.0165(11)	0.0217(11)	0.0205(11)	0.0026(9)	0.0025(8)	0.0055(9)
O(4)	0.0220(4)	0.3765(3)	0.6176(3)	0.0228(5)	0.0159(11)	0.0254(12)	0.0254(11)	−0.0014(9)	−0.0035(9)	−0.0062(9)
O(5)	0.0048(4)	0.1546(3)	0.3686(3)	0.0219(5)	0.0169(11)	0.0233(12)	0.0248(11)	−0.0003(9)	0.0040(9)	0.0035(9)
O(6)	0.2539(4)	0.0557(3)	0.1641(2)	0.0188(4)	0.0136(10)	0.0286(12)	0.0145(10)	0.0043(8)	−0.0009(8)	−0.0032(9)
O(7)	0.4720(4)	0.1273(3)	0.3959(2)	0.0201(5)	0.0162(11)	0.0222(11)	0.0213(11)	0.0021(9)	−0.0032(8)	−0.0056(9)
O(8)	0.1909(5)	−0.0929(2)	0.3600(3)	0.0200(5)	0.0214(11)	0.0144(10)	0.0247(11)	0.0054(8)	−0.0042(9)	−0.0035(8)
O(9)	0.2710(5)	0.8701(3)	0.8935(3)	0.0247(5)	0.0160(11)	0.0356(14)	0.0218(11)	0.0014(10)	0.0006(9)	−0.0026(10)
O(10)	0.1377(6)	0.1631(3)	0.8947(3)	0.0310(6)	0.0298(14)	0.0305(14)	0.0333(14)	0.0064(11)	−0.0013(11)	−0.0092(11)
O(11)	0.2305(5)	0.3942(3)	0.1149(3)	0.0275(5)	0.0221(12)	0.0312(14)	0.0300(13)	0.0056(11)	0.0039(10)	0.0012(10)
O(12)	0.3467(6)	0.6878(3)	0.0819(3)	0.0313(6)	0.0354(15)	0.0309(14)	0.0270(13)	0.0018(11)	−0.0031(11)	0.0095(12)
H(1)	0.436(6)	0.912(7)	0.877(7)	0.084(8)*						
H(2)	0.203(12)	0.819(7)	0.805(4)	0.084(8)*						
H(3)	0.135(13)	0.260(3)	0.947(6)	0.084(8)*						
H(4)	0.112(13)	0.156(7)	0.793(1)	0.084(8)*						
H(5)	0.075(7)	0.449(6)	0.133(7)	0.084(8)*						
H(6)	0.273(13)	0.360(7)	0.205(4)	0.084(8)*						
H(7)	0.320(13)	0.764(5)	0.022(6)	0.084(8)*						
H(8)	0.420(12)	0.717(7)	0.176(3)	0.084(8)*						

* constrained to be equal during refinement

TABLE 3. Selected interatomic distances (Å) and angles (º) for zigrasite.

P(1)−O(1)	1.534(3)	*P*(2)−O(5)	1.537(2)		
P(1)−O(2)	1.522(2)	*P*(2)−O(6)	1.527(2)		
P(1)−O(3)	1.539(2)	*P*(2)−O(7)	1.524(2)		
P(1)−O(4)	1.530(2)	*P*(2)−O(8)	1.542(2)		
<*P*(1)−O>	1.531	<*P*(2)−O>	1.533		
Zr(1)−O(1)	2.056(3)	*Mg*(1)−O(6),d	2.060(2) × 2		
Zr(1)−O(3)a	2.069(2)	*Mg*(1)−O(9)b,e	2.093(3) × 2		
Zr(1)−O(4)b	2.036(2)	*Mg*(1)−O(10)f,g	2.073(3) × 2		
Zr(1)−O(5)b	2.088(2)	<*Mg*(1)−O>	2.075		
Zr(1)−O(7)a	2.059(2)				
Zr(1)−O(8)c	2.090(2)	*Mg*(2)−O(2)a,f	2.038(2) × 2		
<*Zr*−O>	2.066	*Mg*(2)−O(11),h	2.141(3) × 2		
		Mg(2)−O(12),h	2.016(3) × 2		
		<*Mg*(2)−O>	2.065		
O(9)−H(1)	0.980(1)	H(1)....O(6)a	1.735(15)	O(9)−H(1)....O(6)a	167(6)
O(9)−H(2)	0.980(1)	H(2)...O(5)b	2.02(4)	O(9)−H(2)...O(5)b	143(6)
O(10)−H(3)	0.980(1)	H(3)...O(11)i	1.97(4)	O(10)−H(3)−O(11)i	150(6)
		H(3)...O(2)	2.52(6)	O(10)−H(3)...O(2)	123(5)
O(10)−H(4)	0.980(1)	H(4)....O(8)g	2.18(5)	O(10)−H(4)...O(8)g	137(6)
O(11)−H(5)	0.980(1)	H(5)...O(2)b	1.806(14)	O(11)−H(5)...O(2)b	169(6)
O(11)−H(6)	0.980(1)	H(6)...O(6)	2.82(7)	O(11)−H(6)...O(6)	108(5)
O(12)−H(7)	0.980(1)	H(7)...O(9)f	1.698(13)	O(12)−H(7)...O(9)f	169(6)
O(12)−H(8)	0.980(1)	H(8)...O(3)a	1.92(4)	O(12)−H(8)...O(3)a	146(6)

a: 1−*x*, 1−*y*, 1−*z*; b: −*x*, 1−*y*, 1−*z*; c: *x*, 1+*y*, *z*; d: −*x*, −*y*, −*z*; e: *x*, *y*−1, *z*−1; f: *x*, *y*, *z*−1;
g: −*x*, −*y*, 1−*z*; h: 1−*x*, 1−*y*, −*z*; i: *x*, *y*, 1+*z*

that is parallel to (001) and in which alternate tetrahedra point up and down relative to the plane of the sheet. Isolated $Mg(H_2O)_6$ octahedra are arranged in layers parallel to (001).These layers are intercalated between the $[Zr(PO_4)_2]$ sheets, linking through the apical vertices of the (PO_4) tetrahedra (Fig. 2). The structure is formally a heteropolyhedral framework, but the linkage is weaker in the *c* direction, accounting for the marked (001) cleavage.

Hydrogen bonding

Details of the hydrogen bonding are given in Tables 3 and 4, and are illustrated in Fig. 3. The O−H and H...O bond-valences were assigned to bring the incident bond-valence sums close to their ideal values of 2 v.u. that accord with the valence-sum rule (Brown, 1981). Those O anions with lower incident bond-valence sums from P, Mg and Zr (<1.92 v.u., Table 4) are acceptor anions for hydrogen bonds whereas those O anions with greater incident bond-valence sums from P, Mg and Zr (> 1.92 v.u.) do not accept hydrogen bonds (Table 4), confirmation that the arrangement of hydrogen bonds is driven by the valence-sum rule. The majority of the hydrogen bonds are of intermediate strength with bond valences clustered around 0.20 v.u. The exception is the H(6)...O(6) hydrogen bond of 2.67 Å with an assigned bond-valence of 0.05 v.u. (Table 4); O(6) is the only [5]-coordinated O atom (as distinct from H_2O group) in the structure, accepting one stronger hydrogen bond from H(1) and the weak hydrogen bond from O(6) consistent with the valence-sum rule. H(3) forms a bifurcated hydrogen bond to the acceptor anions O(11) and O(2) (Table 3). Note that the hydrogen

TABLE 4. Bond-valence (v.u.) table for zigrasite.

	Zr	*Mg*(1)	*Mg*(2)	*P*(1)	*P*(2)	Σ	H(1)	H(2)	H(3)	H(4)	H(5)	H(6)	H(7)	H(8)	Σ
O(1)	0.71			1.25		1.96									1.96
O(2)			0.39^{x2}↓	1.29		1.68		0.05			0.30				2.03
O(3)	0.68			1.23		1.91								0.15	2.06
O(4)	0.75			1.27		2.02									2.02
O(5)	0.65				1.24	1.89		0.15							2.04
O(6)		0.37^{x2}↓			1.28	1.65	0.30					0.05			2.00
O(7)	0.70				1.29	1.99									1.99
O(8)	0.65				1.22	1.87				0.10					1.97
O(9)		0.34^{x2}↓				0.34	0.70	0.80					0.20		2.04
O(10)		0.36^{x2}↓				0.36			0.85	0.90					2.11
O(11)			0.30^{x2}↓			0.30			0.15		0.70	0.95			2.10
O(12)			0.42^{x2}↓			0.42							0.80	0.85	2.07
Σ	4.14	2.14	2.22	5.04	5.03		1.00	1.00	1.00	1.00	1.00	1.00	1.00	1.00	

bonds to O atoms promote linkage between the different layers of the structure whereas hydrogen bonds to other H_2O groups increase linkage within the layer of Mg octahedra (Fig. 3).

Related minerals

Currently known Zr-phosphate minerals are malhmoodite: $Fe^{2+}Zr(PO_4)_2(H_2O)_4$, Milton *et al.* (1993); kosnarite: $KZr_2(PO_4)_2$, Brownfield *et al.* (1993); wycheproofite: $NaAlZr(PO_4)_2(OH)_2(H_2O)_2$, Kolitsch (2003); and the minerals of the gainsite group (Hawthorne, 1998): gainsite:

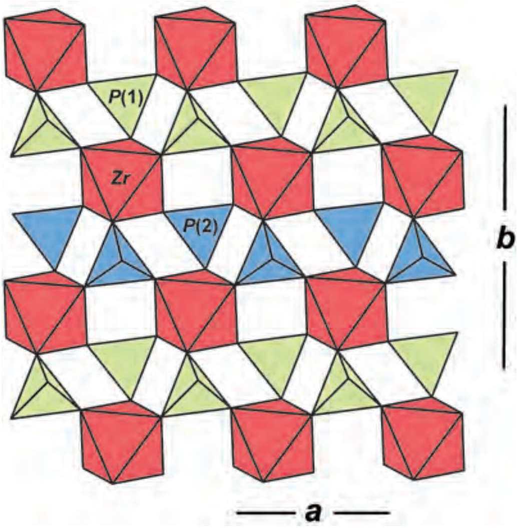

FIG. 1. Details of the crystal structure of zigrasite: the $[Zr(PO_4)_2]$ sheet parallel to (001). Zr octahedra: red; P(1) tetrahedra: green; P(2) tetrahedra: blue.

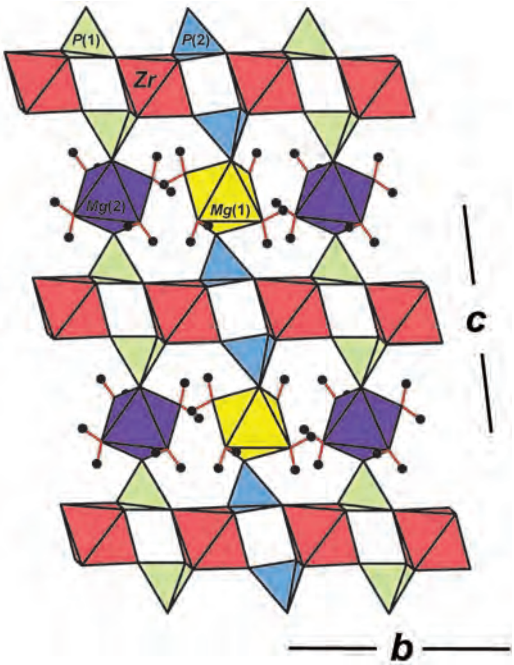

FIG. 2. The crystal structures of zigrasite projected onto (100) showing the $[Zr(PO_4)_2]$ sheets and $Mg(H_2O)_6$ layers edge-on. Legend as in Fig. 1, plus Mg(1) octahedra: yellow; Mg(2) octahedra: purple; H atoms: small black circles; red lines: O–H bonds.

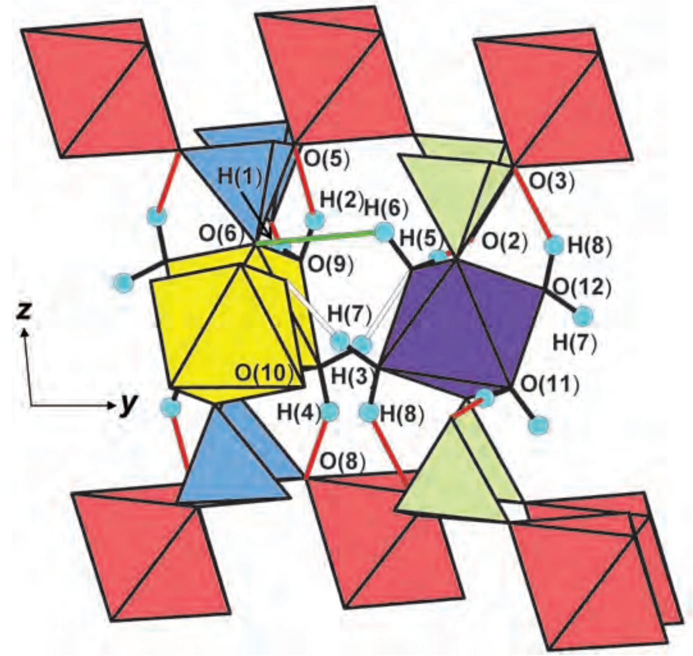

FIG. 3. Arrangement of hydrogen bonds in zigrasite projected down an axis a few degrees from the *a* axis. Legend as in Figs 1 and 2 plus thick black lines: O–H bonds; thick red lines: intermediate-length hydrogen bonds; thick white lines: long hydrogen bonds.

NaK[$BeZr_2(PO_4)_4$], Moore *et al.* (1983); mccrillisite: NaCs[$BeZr_2(PO_4)_4$]$(H_2O)_{1\text{-}2}$, Foord *et al.* (1994); selwynite: NaK[$BeZr_2(PO_4)_4$]$(H_2O)_{1-2}$, Birch *et al.* (1995). The gainsite-group minerals contain (BeO_4) as an oxyanion in addition to (PO_4) and the presence of (BeO_4) strongly affects the bond topology of the resulting structure (Moore *et al.*, 1983). The structure of wycheproofite is dominated by the same [$Zr(PO_4)_2$] sheet (Fig. 4) that occurs in zigrasite (Fig. 1), whereas in kosnarite, the [$Zr(PO_4)_2$] unit is actually a framework.

The [$^{[6]}M(^{[4]}TO_4)_6$] pinwheel cluster is a relatively common feature in a variety of oxysalt structures, and the [$Zr(PO_4)_6$] cluster condenses to form [$Zr(PO_4)_2$] sheets in the structures of zigrasite and wycheproofite. Silicate [$Mg(SiO_4)_6$] and other phosphate [$Mg(PO_4)_6$] analogues occur in the structures of merwinite: $Ca_3[Mg(SiO_4)_2]$, Moore and Araki (1972), Fig. 5*a*; brianite: $Na_2Ca[Mg(PO_4)_2]$, Moore (1975); and yavapaite: K[$Fe^{3+}(SO_4)_2$], Graeber and Rosenweig, (1971), Fig. 5*b*. An isolated [$Fe^{3+}(SO_4)_6$] cluster occurs in ungemachite: $K_3NaFe^{3+}(SO_4)_6(NO_3)_2$ $(H_2O)_6$, Groat and Hawthorne (1986), Fig. 6*a*; and [$Na(SO_4)_6$] clusters link into an [$Na(SO_4)_2$] sheet in glaserite: $K_3Na(SO_4)_2$, Moore (1973), Eysel (1973), and aphthitalite: $K_2NaNa(SO_4)_2$, Okada and Ossaka (1980), Fig. 6*b*. The analogue cluster

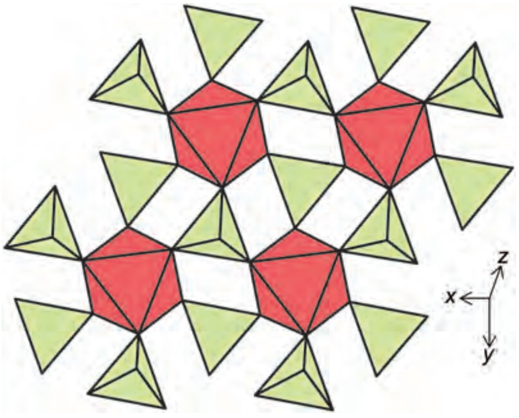

FIG. 4. The [$^{[6]}M(^{[4]}TO_4)_2$] sheet [= $Zr(PO_4)_2$] in wycheproofite; legend as in Fig. 1.

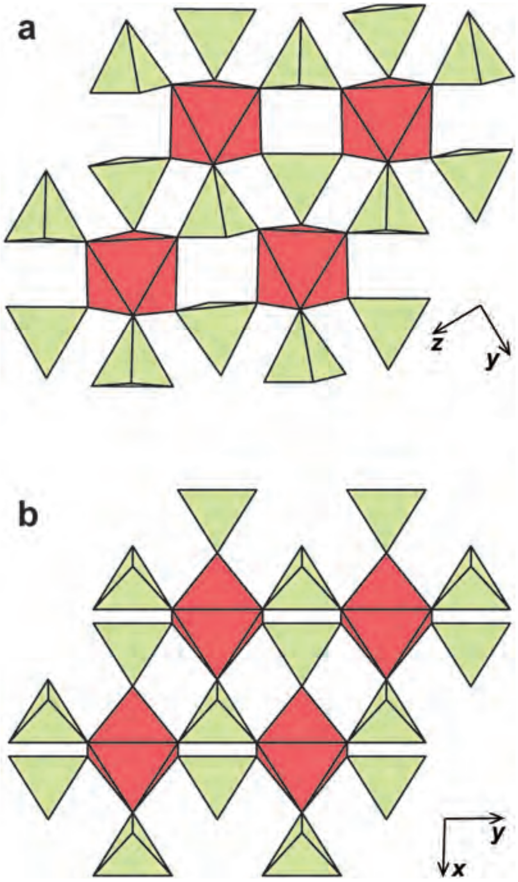

FIG. 5. (*a*) The $[\text{Mg(SiO}_4)_2]$ sheet in merwinite; (*b*) the $[\text{Fe}^{3+}(\text{SO}_4)_2]$ sheet in yavapaiite; legend as in Fig. 1.

$[^{[6]}M(^{[3]}\text{TO}_3)_6]$ contains triangular oxyanions, an example of which occurs in the $[\text{Ca(CO}_3)_2]$ sheet in the minerals of the eitelite group: eitelite, $\text{K}_2[\text{Ca(CO}_3)_2]$, Pabst (1974), Fig. 6*c*; and buetschliite, $\text{K}_2[\text{Ca(CO}_3)_2]$, Pabst (1973).

Malhmoodite

Mahlmoodite, $\text{Fe}^{2+}\text{Zr(PO}_4)_2(\text{H}_2\text{O})_4$, was described as a new mineral species by Milton *et al*. (1993) from the Union Carbide V ore deposit at Wilson Springs, Garland County, Arkansas, USA. Subsequently, Elton and Hooper (1995) described mahlmoodite from Kerriack Cove, near Redruth, Cornwall, England. Grice and Ferraris (2002) reported that mahlmoodite was renamed malhmoodite (IMA Code 02-D) by the

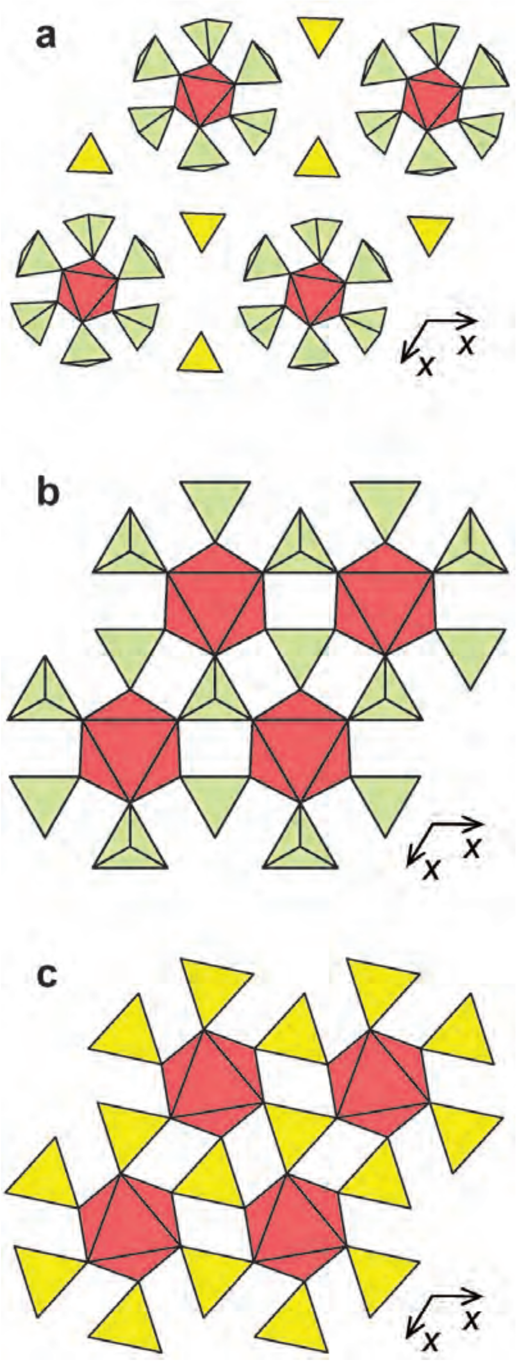

FIG. 6. (*a*) The $[\text{Fe}^{3+}(\text{SO}_4)_6]$ pinwheel cluster in ungemachite; (*b*) the $[\text{Na(SO}_4)_2]$ sheet in aphthitalite; (*c*) the $[\text{Ca(CO}_3)_2]$ sheet in eitelite; legend as in Fig. 1, plus yellow triangles are (TO_3) groups.

Commission on New Minerals and Mineral Names (as it was then known) of the International Mineralogical Association.

Malhmoodite (Milton *et al.*, 1993; Elton and Hooper, 1995) and various synthetic analogues of malhmoodite (Alluli *et al.*, 1976) were described as monoclinic with a doubled unit cell relative to that found here for zigrasite. However, no crystal structures have been reported for these structures. Particular attention was paid to this issue in our experimental work, but there was no trace of reflections indicating a doubled unit cell in the diffraction pattern of zigrasite. More than a sphere of data was collected and all data merge well in triclinic Laue symmetry (R_{merge} = 1.4%). If the data is indexed on a malhmoodite-like cell (obviously much of the data is not observed), merging the data in monoclinic Laue symmetry gives an R_{merge} of 29.9%. We also refined the cell dimensions from 6768 reflections with $I > 10\sigma I$ in both triclinic and monoclinic geometries with a cell metrically similar to that given for malhmoodite, and the results are compared in Table 5. Although the fit for the monoclinic cell looks reasonable for powder-pattern data, it is much poorer than the fit for the triclinic cell and much poorer than fits usually are for single-crystal CCD data. The above triclinic cell has a volume exactly twice that of the triclinic cell given in Table 1: 472.79 × 2 = 945.58 Å^3 (see Table 5); the two triclinic cells are related by the transformation matrix 010 /100/002. However, the cell volume for monoclinic symmetry differs by 17.2 Å^3 from the corresponding value with triclinic symmetry, suggesting that the monoclinic constraint is resulting in an erroneous cell volume. Thus we conclude that zigrasite is truly triclinic (and only pseudo-metrically monoclinic).

TABLE 5. Comparison of cell dimensions of zigrasite refined in triclinic and monoclinic symmetries in the setting used previously for malhmoodite.

	Triclinic	Monoclinic
a (Å)	9.3372(4)	9.392(5)
b	5.3048(2)	5.335(3)
c	19.2560(8)	19.379(11)
α (°)	88.466(1)	90
β	97.347(1)	97.43(1)
γ	89.488(1)	90
V (Å^3)	945.55(11)	963(2)

Acknowledgements

The authors thank Alexander Hölzel (Germany) and Jacques LaPaire (Switzerland) for bringing the issue of malhmoodite to our attention, and Mark Cooper and Al Falster for technical help. This work was funded by a Canada Research Chair in Crystallography and Mineralogy, and by a Major Facilities Access Grant, Research Tools and Equipment, and Discovery Grants to FCH from the Natural Sciences and Engineering Research Council of Canada, and by Canada Foundation for Innovation Grants to FCH.

References

Alluli, G., Ferragina, C., La Ginestra, A., Massucci, M.A., Tomssini, N. and Tomlinson, A.A.G. (1976) Characterization and electronic properties of inorganic ion exchangers of the zirconium phosphate type containing transition metal ions. *Journal of the Chemical Society, Dalton Transactions*, 2115–2120.

Birch, W.D., Pring, A. and Foord, E.E. (1995) Selwynite, NaK(Be,Al)Zr$_2$(PO$_4$)$_4$.2H$_2$O, a new gainesite-like mineral from Wycheproof, Victoria, Australia. *The Canadian Mineralogist*, **33**, 55–58.

Brown, I.D. (1981) The bond-valence method: an empirical approach to chemical structure and bonding. Pp. 1–30 in: *Structure and Bonding in Crystals II* (M. O'Keeffe and A. Navrotsky, editors). Academic Press, New York.

Brownfield, M.E., Foord, E.E., Sutley, S.J. and Botinelly, T. (1993) Kosnarite, KZr$_2$(PO$_4$)$_3$, a new mineral from Mount Mica and Black Mountain, Oxford County, Maine. *American Mineralogist*, **78**, 653–656.

Elton, N.J. and Hooper, J.J. (1995) A second occurrence of mahlmoodite, from Cornwall, England. *Mineralogical Magazine*, **59**, 166–168.

Eysel, W. (1973) Crystal chemistry of the system Na$_2$SO$_4$-K$_2$SO$_4$-K$_2$CrO$_4$-Na$_2$CrO$_4$, and of the glaserite phase. *American Mineralogist*, **58**, 736–747.

Foord, E.E., Brownfield, M.E., Lichte, F.E., Davis, A.M. and Sutley, S.J. (1994) Mccrillisite, NaCs(Be,Li)Zr$_2$(PO$_4$)$_4$·1-2H$_2$O, A new mineral species from Mount Mica, Oxford County, Maine, and new data for gainesite. *The Canadian Mineralogist*, **32**, 839–842.

Graeber, E.J. and Rozenweig, A. (1971) The crystal structures of yavapaiite, KFe(SO$_4$)$_2$, and goldichite, KFe(SO$_4$)$_2$.4H$_2$O. *American Mineralogist*, **56**, 1917–1936.

Grice, J.D. and Ferraris, G. (2002) New minerals approved in 2002: Nomenclature modifications approved 1998–2002 by the Commission on New

Minerals and Mineral Names, International Mineralogical Association. *Mineralogy and Petrology*, **80**, 97–110.

Groat, L.A. and Hawthorne, F.C. (1986) Structure of ungemachite, $K_3Na_8Fe_{3+}(SO_4)_6(NO_3)_2.6(H_2O)$, a mixed sulfate-nitrate mineral. *American Mineralogist*, **71**, 826–829.

Hawthorne, F.C. (1998) Structure and chemistry of phosphate minerals. *Mineralogical Magazine*, **62**, 141–164.

Hawthorne, F.C., Ball, N.A., Nizamoff, J.W. and Simmons, W.B. (2009) Zigrasite, $MgZr(PO_4)_2(H_2O)_4$, a new phosphate mineral from the Dunton Quarry, Newry, Oxford County, Maine, U.S.A. *Mineralogical Magazine*, **73**, 415–420.

Huminicki, D.M.C. and Hawthorne, F.C. (2002) The crystal chemistry of the phosphate minerals. Pp. 123–253 in: *Phosphates: Geochemical, Geobiological, and Materials Importance* (M.J. Kohn, J. Rakovan and J.M. Hughes, editors). Reviews in Mineralogy and Geochemistry, **48**, Mineralogical Society of America, Washington D.C. and the Geochemical Society, St. Louis, Missouri, USA.

International Tables for X-ray Crystallography (1992) Kluwer Academic Publishers, V.C. Dordrecht, The Netherlands.

Kolitsch, U. (2003) The crystal structure of wycheproofite, $NaAlZr(PO_4)_2(OH)_2{\cdot}(H_2O)$. *European Journal of Mineralogy*, **15**, 1029–1034.

Milton, C., McGee, J.J. and Evans Jr., H.T. (1993) Mahlmoodite, $FeZr(PO_4)_2.4H_2O$, a new iron zirconium phosphate mineral from Wilson Springs, Arkansas. *American Mineralogist*, **78**, 437–440.

Moore, P.B. (1973) Bracelets and pinwheels: a topological-geometrical approach to the calcium orthosilicate and alkali sulfate structures. *American Mineralogist*, **58**, 32–42.

Moore, P.B. (1975) Brianite, $Na_2CaMg[PO_4]_2$: a phosphate analog of merwinite, $Ca_2CaMg[SiO_4]_2$. *American Mineralogist*, **60**, 717–718.

Moore, P.B. and Araki, T. (1972) Atomic arrangement of merwinite, $Ca_3Mg[SiO_4]_2$, an unusual dense-packed structure of geophysical interest. *American Mineralogist*, **57**, 1355–1374.

Moore, P.B. Araki, T., Steele, I.M., Swihart, G.H. and Kampf, A.R. (1983) Gainesite, sodium zirconium beryllophosphate: a new mineral and its crystal structure. *American Mineralogist*, **68**, 1022–1028.

Okada, K. and Ossaka, J. (1980) Structures of potassium sodium sulphate and tripotassium sodium disulphate. *Acta Crystallographica*, **B24**, 919–921.

Pabst, A. (1973) The crystallography and structure of eitelite, $Na_3Mg(CO_3)_2$. *American Mineralogist*, **58**, 211–217.

Pabst, A. (1974) Synthesis, properties and structure of $K_2Ca(CO_3)_2$, buetschliite. *American Mineralogist*, **59**, 353–358.

Sheldrick, G.M. (1997) *SHELX-97: Program for the solution and refinement of crystal structures*. Siemens Energy and Automation, Madison, Wisconsin, USA.

Sheldrick, G.M. (1998) *SADABS User Guide*, University of Göttingen, Germany.